

CD4–T-cell antigen receptor complexes on human leukemia T cells

(receptors/molecular assemblies/flow cytometry/energy transfer)

ROY S. CHUCK*†‡§, CHARLES R. CANTOR†‡§, AND DORIS B. TSE*¶

*Laboratory of Lymphocyte Cell Biology, Department of Medicine, North Shore University Hospital–Cornell University Medical College, Manhasset, NY 11030; †Department of Genetics and Development, Columbia University, New York, NY 10032; and ‡Department of Molecular and Cell Biology, University of California, Berkeley, CA 94720

Contributed by Charles R. Cantor, April 19, 1990

ABSTRACT CD4 and T-cell antigen receptor (TCR) co-modulate from the surface of human and murine T cells following exposure to monoclonal anti-CD4 or anti-TCR. This co-modulation may occur because expression of CD4 and TCR is regulated by similar transmembrane signals or because CD4 and TCR are physically associated. To study multimolecular assemblies on the plasma membrane, we developed a flow cytometric method for detecting singlet-singlet energy transfer between fluorescein isothiocyanate (FITC)- and tetramethylrhodamine isothiocyanate (TRITC)-conjugated monoclonal antibodies as sensitized TRITC emission on intact, single cells. Using this procedure, we detected CD4–TCR complexes on the surface of the transformed human leukemia T cells, HPB-ALL, in the absence of stimulation. More than one CD4 were found in association with one TCR. CD4–TCR complexes were not in rapid equilibrium with free CD4 and free TCR, and they were not induced by the dye-labeled anti-CD4 or anti-TCR.

CD4 is an invariant 55-kDa surface receptor (1). Its expression on T lymphocytes is tightly associated with their restriction to class II major histocompatibility complex (MHC) antigens (2). CD4 binds directly to monomorphic determinants on class II MHC antigens (3). It is capable of transmembrane signaling (4), and it is associated with a protein tyrosine kinase on the plasma membrane (5, 6). Considerable evidence shows that CD4 interacts with T-cell antigen receptor (TCR) and that proximity of CD4 to TCR is closely associated with T-cell activation. When T lymphocytes interact with cells presenting specific antigen in the context of class II MHC molecules, CD4 and TCR are localized within the region of cell–cell contact (7). Antigenic stimulation of T cells causes a parallel decrease in the cell surface expression of CD4 and TCR (8, 9). T lymphocytes stimulated with anti-CD4 and anti-TCR immobilized on the same insoluble support invariably gave higher responses than T lymphocytes stimulated with mixtures of separately immobilized anti-CD4 and anti-TCR (10, 11). Anti-TCR modulated CD4 as well as TCR from the T-cell surface. Likewise, anti-CD4 modulated TCR as well as CD4 (12, 13). Furthermore, the capacity of different anti-TCR monoclonal antibodies (mAbs) to induce CD4–TCR association correlated with the stimulatory potential of these serological reagents (14, 15). However, all of the studies described required exposure of T cells to conditions that allow for receptor mobilization and aggregation within the plasma membrane (7–16). Thus, none of this evidence shows whether CD4–TCR complexes are present on the cell surface prior to TCR cross-linking and TCR-mediated T-cell triggering.

There is recent biochemical evidence that a small proportion of TCR is associated with CD4 on the surface of murine T-cell clones in the absence of *in vivo* activation (17). We

have developed a flow cytometric method to detect singlet-singlet energy transfer on cells labeled with fluorescent dye pairs coupled to mAbs. Using this method we now show that CD4–TCR complexes preexist on the surface of transformed human leukemia T cells as stable molecular assemblies.

MATERIALS AND METHODS

Cells. The human leukemia T-cell line HPB-ALL was propagated in Iscove's modified Dulbecco's medium supplemented with 10% fetal calf serum (FCS), 100 units of penicillin per ml, 100 μ g of Fungizone per ml, 50 μ g of gentamicin per ml, and 20 mM glutamine. FCS was obtained from HyClone. All other tissue culture reagents were obtained from GIBCO. Only cells in the exponential phase of growth were used in these experiments.

Antibodies. Hybridoma T40/25, which recognizes an idiotypic determinant on the $\alpha\beta$ receptor of HPB-ALL, was the gift of I. Trowbridge (Salk Institute, San Diego, CA). Hybridomas OKT3 and OKT4 were obtained through B. Pernis (Columbia University). Hybridoma GA2 was the gift of C. Russo (Cornell University Medical College). mAbs were purified either from culture supernatant by affinity chromatography over protein A-Sepharose or by ammonium sulfate fractionation from ascitic fluid.

Immunofluorescence. Fluorescein isothiocyanate (FITC) and tetramethylrhodamine isothiocyanate (TRITC) were purchased from Sigma. Antibodies were conjugated directly to FITC and TRITC as described (18). The fluorophore-to-protein ratio was determined from the A_{488}/A_{280} ratio for FITC conjugates and the A_{568}/A_{280} ratio for TRITC conjugates.

HPB-ALL cells were removed from culture, washed with chilled Hanks' balanced salt solution containing 10 mM Hepes buffered to pH 7.4 (HBSS), and supplemented with 5% FCS; cells were then allowed to react at 0°C for 30 min with mAb at a pretitered concentration. Following this, cells were washed twice with HBSS/FCS at 0°C and resuspended in chilled HBSS/FCS and 10 mM NaN_3 for flow cytometric analyses.

Flow Cytometry. Cells were analyzed using a Becton Dickinson FACS440 cell sorter equipped to monitor five parameters. Dual argon and krypton lasers were used for excitation at 488 nm and 568 nm, respectively. Forward scattered light of 488 nm was collected through a neutral density filter (parameter 1) and light scattered at 90° was collected through a 488/10-nm band pass filter (parameter 4). Emitted light was detected at 90° to the laser beam. FITC

Abbreviations: FCS, fetal calf serum; FITC, fluorescein isothiocyanate; mAb, monoclonal antibody; MHC, major histocompatibility complex; TCR, T-cell antigen receptor; TRITC, tetramethylrhodamine isothiocyanate; S'TRITC, sensitized TRITC.

§Present address: Department of Molecular and Cell Biology, University of California, Berkeley, CA 94720.

¶To whom reprint requests should be addressed.

The publication costs of this article were defrayed in part by page charge payment. This article must therefore be hereby marked "advertisement" in accordance with 18 U.S.C. §1734 solely to indicate this fact.

fluorescence was excited at 488 nm and collected through a 530/30-nm band pass filter after reflection by a 560-nm dichroic mirror (parameter 2). TRITC fluorescence was excited at 568 nm and collected as a delayed signal through a 630/22-nm band pass filter (parameter 3). Sensitized TRITC (S'TRITC) emission was excited at 488 nm and collected through a 560-nm dichroic mirror and a 590-nm long pass filter (parameter 5). Thorn EMI model 4001-06-300 photomultiplier tubes were used for measuring fluorescence. There was no detectable spillover of FITC fluorescence into parameter 3 or TRITC fluorescence into parameter 2. All measurements were collected in list mode and subsequently analyzed on a Digital microVaxII using Consort 40 software (Becton Dickinson). Forward and 90° light scatter were used to select live cells.

Calculations. Fluorescence intensity measured by logarithmic amplification of detected signals was linearized using the formula

$$F = 10^{(x/60/G)}, \quad [1]$$

where F = fluorescence intensity, x = log fluorescence intensity in channel numbers, and G = photomultiplier gain or amplification ratio.

$F_i(X)$ is defined such that i = parameter number as described above, and $X = D, A,$ or $D + A$ indicating, respectively, samples labeled with donor only, acceptor only, or donor and acceptor. $\langle F \rangle$ indicates the mean fluorescence intensity for a population of cells and F represents single cell measurements. $\langle F_i \rangle$ for each parameter is independently corrected to remove contributions from autofluorescence by subtracting the corresponding mean fluorescence intensity measured on unlabeled cells. S'TRITC emission, corrected for spillover from D and A into parameter 5, is given by:

$$F'_5(D + A) = F_5(D + A) - F_2(D + A) \frac{\langle F_5(D) \rangle}{\langle F_2(D) \rangle} - F_3(D + A) \frac{\langle F_5(A) \rangle}{\langle F_3(A) \rangle}. \quad [2]$$

For samples saturated with D and A , single cell energy transfer efficiency can be estimated as:

$$E = \frac{F'_5(D + A) \langle F_2(D) \rangle}{F_2(D + A) \langle F_5(D) \rangle \left[\frac{f(A)a(D)}{f(D)a(A)} - 1 \right]}, \quad [3]$$

where a and f refer, respectively, to the absorbance at 488 nm and the 488-nm-excited, integrated fluorescence at wavelengths >590 nm measured for donor or acceptor labeled cells in suspension.

RESULTS

Physical Association of CD4 and TCR Detected by Flow Cytometric Energy Transfer. The ability of flow cytometric energy transfer to detect the physical association of two distinct glycoproteins on the cell surface was first confirmed for CD3 and TCR, since this multimolecular complex has been unequivocally identified on murine and human T cells by biochemical techniques (19). Anti-CD3 mAb conjugated to FITC (FITC-OKT3) was selected as the donor and TRITC-T40/25 was selected as the acceptor. HPB-ALL cells were simultaneously labeled under saturating conditions at 0°C with FITC-OKT3 and TRITC-T40/25 and then analyzed as described in *Materials and Methods*. Typical histograms of fluorescence recorded for parameters 2, 3, and 5 are shown in Fig. 1A, panel *i*. It is important to note that intensities are

shown on a logarithmic scale. Thus the emission shift in the donor and acceptor labeled sample detected on parameter 5 represents quite significant energy transfer. However, donor quenching was not detected on parameter 2, for unknown reasons. S'TRITC emission was determined as described in *Materials and Methods*. Positive cells are shown in Fig. 1B, panel *i*.

We next saturated HPB-ALL cells using the same mAb, GA2, separately conjugated to FITC and TRITC. GA2 recognizes a monomorphic determinant on HLA-A,B antigens. Fluorescence histograms are shown in Fig. 1A, panel *ii*. The large decrease in donor fluorescence detected on parameter 2 for the donor and acceptor labeled sample was mostly the result of binding competition, which would obscure any evidence of donor quenching commensurate with the small emission shift detected on parameter 5. As indicated by the small number of positive cells and considerably lower S'TRITC intensity (relative to that observed for the FITC-OKT3 and TRITC-T40/25 dye pair) in Fig. 1B, we can conclude that very few FITC-GA2 and TRITC-GA2 were in close proximity to each other. Low levels of energy transfer between FITC and TRITC conjugated to mAbs directed against class I MHC antigens have been reported by other investigators for murine (20) and human T lymphocytes (21).

We then saturated HPB-ALL cells at 0°C simultaneously with FITC-OKT4 (anti-CD4) and TRITC-T40/25. As seen in Fig. 1A, panel *iii*, an emission shift for the donor and acceptor labeled sample was detected on parameter 5, whereas corresponding donor quenching was detected on parameter 2. Since donor quenching was not observed on cells saturated with FITC-OKT4 and unlabeled T40/25, it must be related to the presence of an energy acceptor on TRITC-T40/25. As shown in Fig. 1B, the number of cells positive for S'TRITC was considerably higher than that detected for the FITC-GA2 and TRITC-GA2 dye pair. On the other hand, the intensity of S'TRITC emission was significantly lower than that observed for the FITC-OKT3 and TRITC-T40/25 dye pair. The molar ratio of fluorophore to protein was almost equivalent for FITC-OKT4 (fluorophore-to-protein ratio = 1.0) and FITC-OKT3 (fluorophore-to-protein ratio = 1.1). However, on donor labeled cells (Fig. 1A, parameter 2), $\langle F_2(D + A) \rangle$ for FITC-OKT3 (mean = 84) was nearly 2-fold that for FITC-OKT4 (mean = 45). The ratio, $\langle F_2(D) \rangle / \langle F_5(D) \rangle$, is constant for the same dye. Thus, the efficiency of energy transfer (estimated using Eq. 3) is actually higher for the FITC-OKT4 and TRITC-T40/25 dye pair. This means that the T40/25-reactive idiotype determinant may be closer to the OKT4-reactive epitope than the OKT3-reactive epitope. On the other hand, the number of cells positive for S'TRITC is significantly lower compared to the FITC-OKT3 and TRITC-T40/25 dye pair. This implies that, similar to murine T-cell clones (17), considerably fewer CD4 molecules, relative to CD3 molecules, may be in close proximity to TCR molecules on the surface of HPB-ALL cells.

Since energy transfer in the present experiment was detected on prechilled cells stained and kept at 0°C in the presence of NaN_3 , it is unlikely that the physical association of CD4 and TCR was induced by the mAbs used to detect their presence. These CD4-TCR complexes, more likely, preexisted on the surface of HPB-ALL cells.

CD4-TCR Complexes Were Not Dependent on the Density of the Free Molecules and Were Not Induced by Antibodies. Since samples were stained under saturating conditions for FITC-OKT4 and TRITC-T40/25, the magnitude of donor and acceptor fluorescences should measure the density of the respective molecules on the surface of *single* cells. To determine if the number of CD4-TCR complexes was governed by the density of the individual receptors on the cell surface, list mode data files were reprocessed so that subsets of cells displaying low, median, and high levels of CD4 could

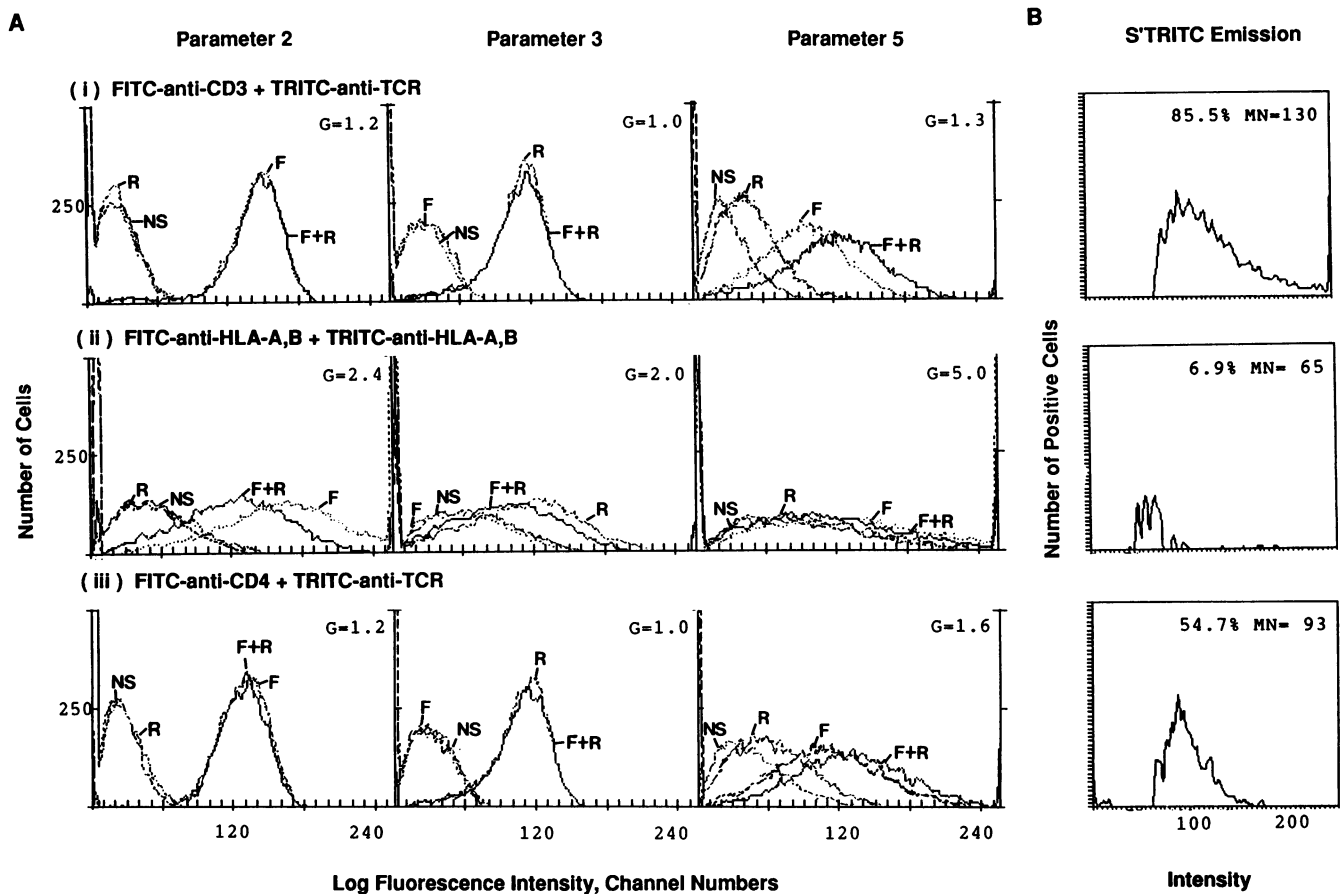


FIG. 1. Detection of energy transfer between (i) FITC-OKT3 and TRITC-T40/25, (ii) FITC-GA2 and TRITC-GA2, and (iii) FITC-OKT4 and TRITC-T40/25. HPB-ALL cells were stained at 0°C simultaneously with FITC-mAb and TRITC-mAb. Controls include unstained cells (NS), cells stained with only FITC-mAb (F), and cells stained with only TRITC-mAb (R). Cells were analyzed at 0°C. (A) List mode data recorded on parameters 2 (excitation, 488 nm; emission, 515–545 nm), 3 (excitation, 568 nm; emission, 620–640 nm), and 5 (excitation, 488 nm; emission, >590 nm). G = photomultiplier gain. (B) Data processed to determine S'TRITC emission. Positive cells were obtained after channel-by-channel subtraction of autofluorescent cells (mean intensity = 52) detected on parameter 5. Percent positive cells and mean S'TRITC intensity (MN) are given in each histogram. This experiment is representative of three others.

be examined. When cells expressing low and high levels of CD4 are compared (Fig. 2 Upper), there is a 4-fold difference in the intensity of donor fluorescence but only a slight increase (11%) in the intensity of S'TRITC emission. Similarly, when subsets of cells expressing low and high levels of TCR are compared (Fig. 2 Lower), there is a 5-fold difference in acceptor intensity but only a relatively slight increase (14%) in S'TRITC intensity, even though there is a correlated 64% increase in donor intensity. This argues against weak or transient bimolecular interactions of free CD4 and free TCR molecules within the lipid bilayer as the principal mechanism regulating the expression of CD4-TCR complexes. Since more TRITC-T40/25 bound per cell did not result in proportionally higher S'TRITC emission, the observed CD4-TCR complexes are unlikely to result from CD4-TCR association induced by the anti-TCR mAb used in our experiments.

More Than One CD4 Molecule Associate with One TCR. To determine the limits of detection in our flow cytometric analyses of S'TRITC emission, HPB-ALL cells were first saturated with TRITC-T40/25 and then allowed to react with decreasing concentrations of FITC-OKT4. S'TRITC emission decreased with decreasing donor fluorescence (correlation coefficient = 1.00) and could still be detected at donor levels 10% that of saturation (Fig. 3A). When HPB-ALL cells were first saturated with FITC-T40/25 and then allowed to react with decreasing concentrations of TRITC-T40/25, S'TRITC emission decreased with decreasing acceptor fluorescence (correlation coefficient = 0.96) and could be

detected at acceptor levels 20% that of saturation (Fig. 3B). This apparent decrease in sensitivity was not dependent on the detection of S'TRITC emission but was caused, instead, by lower signal-to-noise ratios encountered in the detection of reduced levels of TRITC fluorescence excited at 568 nm.

Although S'TRITC emission decreased linearly with acceptor fluorescence, marked deviation from linearity is observed with donor fluorescence. No gross heterogeneity in labeling is observed when FITC and TRITC fluorescence intensities are examined at concentrations of FITC-OKT4 and TRITC-T40/25 below saturation (Fig. 3 Insets). Most significantly, polynomial curve fitting analysis of S'TRITC emission showed linear dependence on acceptor fluorescence and quadratic dependence on donor fluorescence with a proportionality constant of one for both (0.98 and 0.99, respectively; Fig. 3, equations). The simplest interpretation is that more than one FITC-OKT4 binding site were located in the vicinity of each TRITC-T40/25 binding site—that is, more than one CD4 molecule associate with each TCR molecule.

DISCUSSION

CD4 and TCR comodulate from the surface of human and murine T cells following engagement of either CD4 or TCR (12, 13). Although these data suggest that a direct complex of CD4 and TCR might exist in significant numbers, it is impossible to use these observations alone as evidence for

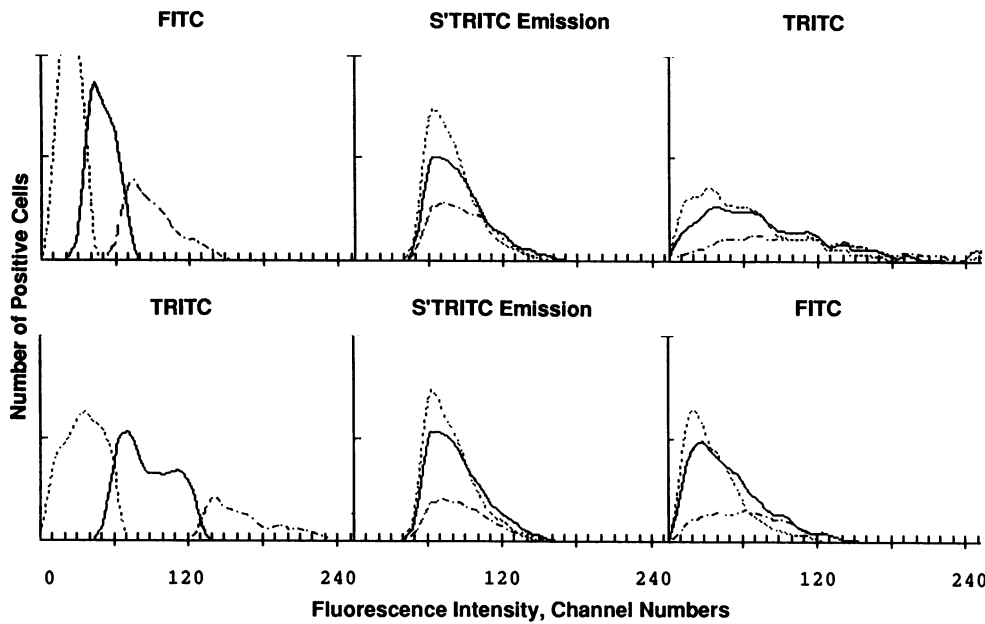


FIG. 2. Effect of CD4 and TCR density on CD4-TCR complexes. Data collected on HPB-ALL cells stained with FITC-OKT4 and TRITC-T40/25 were reprocessed. (Upper) Cells were gated on the bases of low (—), median (---), or high (···) donor intensity. Mean intensities corresponding to low, median, and high donor subsets are 23, 50, and 94 for FITC; 79, 86, and 88 for S'TRITC; and 64, 81, and 110 for TRITC. (Lower) Cells were gated on the bases of low (—), median (---), or high (···) acceptor intensity. Mean intensities corresponding to low, median, and high acceptor subsets are 35, 89, and 178 for TRITC; 79, 85, and 90 for S'TRITC; and 39, 50, and 64 for FITC.

the presence of CD4-TCR complexes. Exposure of either CD4 or TCR to reactive antibodies causes mobilization of intracellular Ca^{2+} and activation of protein kinases that regulate the expression of CD4 and TCR on the cell surface (4, 5, 22-25). Thus, it is impossible to ascertain if comodulation is the result of physically associated CD4 and TCR or heterologous down-regulation as described for functionally unrelated surface receptors on nonlymphoid cells (26).

To overcome the ambiguities just described, we have performed flow cytometric analyses of nonradiative energy transfer between donor labeled anti-CD4 and acceptor labeled anti-TCR. Although singlet-singlet energy transfer measurements in principle can reveal the actual distance

between fluorescent dyes (27), the interpretation of such measurements for macromolecular cell surface assemblies is complicated by the indirect modes of chromophore attachment and the dynamic nature of the plasma membrane. Thus, the apparent distribution of distances between donor and acceptor can reflect the distribution of the labeled epitopes or the distribution of the antibodies used to identify the molecules within the putative assembly (28). The latter is governed by the rigidity of the antibody combining sites, the freedom of rotation at the hinge, the site of chromophore attachment, and the orientation of the antibodies with respect to each other. Therefore, although undetectable energy transfer is not conclusive evidence for lack of association, any

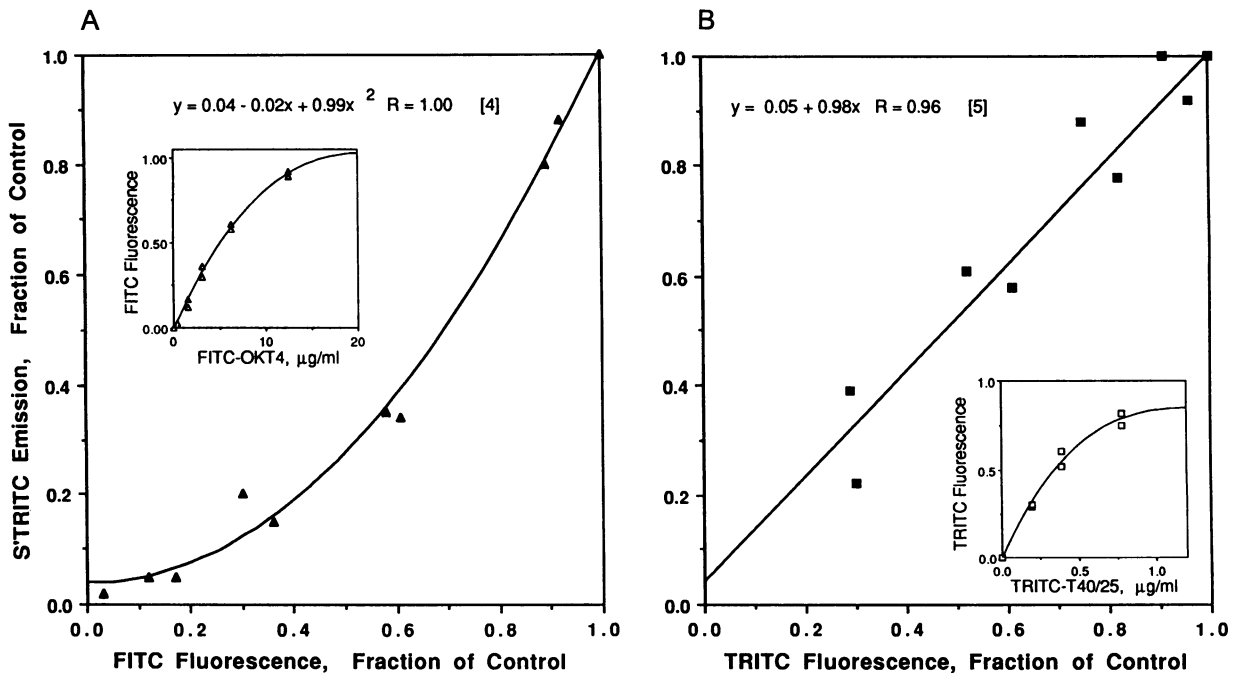


FIG. 3. Effect of decreasing FITC-OKT4 and TRITC-T40/25 labeling on S'TRITC emission. (A) HPB-ALL cells were stained simultaneously at 0°C with TRITC-T40/25 under saturating conditions and with FITC-OKT4 under saturating conditions at $25\ \mu\text{g}/\text{ml}$ (control) or subsaturating conditions. FITC and S'TRITC intensities were given by $\langle F_2(D+A) \rangle$ and $\langle F'_5(D+A) \rangle$. (B) HPB-ALL cells were stained simultaneously at 0°C with FITC-OKT4 under saturating conditions and with TRITC-T40/25 under saturating conditions at $5\ \mu\text{g}/\text{ml}$ (control) or subsaturating conditions. TRITC and S'TRITC intensities were given by $\langle F_3(D+A) \rangle$ and $\langle F'_5(D+A) \rangle$. Results were obtained from two separate experiments. R = correlation coefficient.

energy transfer detected using this technology is fairly solid evidence for proximity between two epitopes on the cell surface. The width of the Fab fragment is estimated to be $35 \pm 10 \text{ \AA}$ (29). Thus a minimum distance of 25–45 \AA separates the OKT4 and T40/25 epitope. Assuming freely rotating donors and acceptors, the characteristic distance, $R_0(2/3)$, for the FITC and TRITC dye pair used is 40 \AA (27). In the most extreme case where donor and acceptor are carried on the domain most distal to the combining site and the antibodies are oriented directly toward each other, a distance of six antibody domains or 150 \AA could theoretically separate the OKT4 and T40/25 epitope and still allow nonradiative energy transfer to occur. In practice, it is far more likely that the epitopes are considerably closer.

A third level of complexity is produced if the plasma membrane and its associated cytoskeletal structures are perturbed during the energy transfer measurements. Transmembrane signals triggered by reactive antibodies can alter glycoprotein movements within the lipid bilayer and affect distance distributions between donor and acceptor (30, 31). Since these changes cannot be detected with fluorescent labels in the light microscope (32), energy transfer observed under these conditions could be misinterpreted as direct molecular interactions between the labeled surface glycoproteins. In our studies, energy transfer was detected (as S'TRITC emission) on T cells exposed to FITC-anti-CD4 and TRITC-anti-TCR at 0°C in the presence of sodium azide. Therefore, the CD4-TCR complexes observed cannot result from molecular movements produced by cytoskeletal mechanisms. This conclusion is also supported by the observation that S'TRITC intensity does not correlate with donor or acceptor intensity on a cell-by-cell basis. Since the CD4-TCR complexes detected are not governed by the surface density of CD4 or TCR, they cannot be simple bimolecular reaction products of the free receptors. Furthermore, since they are detected on the plasma membrane of transformed T cells that do not express class II MHC antigens, these complexes represent a stable cellular phenotype rather than the transient product of reactions that take place during cognate T-cell and antigen-presenting cell interaction. Since energy transfer between FITC-anti-CD4 and TRITC-anti-CD3 was also detected on interleukin 2-dependent human T-cell clones (R.S.C., S. Friedman, and D.B.T., unpublished observations), CD4-TCR complexes are not unique to transformed human T cells.

Our analysis of S'TRITC emission as a function of decreasing epitope saturation shows that more than one CD4 are associated with one TCR within a single molecular assembly. A receptor complex consisting of more than one monomeric binding site and one antigen-specific binding site will undoubtedly have greater avidity for peptide-presenting class II MHC antigens than the antigen-specific receptor alone (33). Exposure of CD4 to the human immunodeficiency virus (HIV) envelope glycoprotein gp120 results in the inhibition of T helper cell function but does not result in CD4 down-regulation (34–36). Engagement of CD4 by anti-CD4, or gp120, may disrupt preformed CD4-TCR complexes and block the *in situ* association of CD4 and TCR during cognate T-cell-presenter cell interaction. This can account for CD4-mediated negative signaling to T cells (11, 37). It also poses another mechanism for the disruption of T-cell immunity by the HIV (1).

We thank Benvenuto Pernis for his suggestion to use singlet-singlet energy transfer for studying interactions between lymphocyte surface molecules and Paul Fischer for his assistance with the calcula-

tions. This work is supported by National Institutes of Health Grants CA39782 and S07RR05924 and a Special Projects Fund from the Department of Medicine, North Shore University Hospital-Cornell University Medical College. R.S.C. is a National Institutes of Health Medical Scientist Trainee.

- Littman, D. R. (1987) *Annu. Rev. Immunol.* **5**, 561–584.
- Meuer, S. C., Acuto, O., Hercend, T., Schlossman, S. F. & Reinherz, E. L. (1984) *Annu. Rev. Immunol.* **2**, 23–50.
- Gay, D., Buus, S., Pasternak, J., Kappler, J. & Marrack, P. (1988) *Proc. Natl. Acad. Sci. USA* **85**, 5629–5633.
- Ledbetter, J. A., June, C. H., Grosmaire, L. S. & Rabinovitch, P. S. (1987) *Proc. Natl. Acad. Sci. USA* **84**, 1384–1388.
- Rudd, C. E., Trevillyan, J. M., Dasgupta, J. D., Wong, L. L. & Schlossman, S. F. (1988) *Proc. Natl. Acad. Sci. USA* **85**, 5190–5194.
- Veillette, A., Bookman, M. A., Horak, E. M., Samelson, L. E. & Bolen, J. B. (1989) *Nature (London)* **338**, 257–259.
- Kupfer, A., Singer, S. J., Janeway, C. A., Jr., & Swain, S. L. (1987) *Proc. Natl. Acad. Sci. USA* **84**, 5888–5892.
- Weyand, C. M., Goronzy, J. & Fathman, C. G. (1987) *J. Immunol.* **138**, 1351–1354.
- Rivas, A., Takada, S., Koide, J., Sonderstrup-McDevitt, G. & Engleman, E. G. (1988) *J. Immunol.* **140**, 2912–2918.
- Anderson, P., Blue, M.-L., Morimoto, C. & Schlossman, S. F. (1987) *J. Immunol.* **139**, 678–682.
- Ledbetter, J. A., June, C. H., Rabinovitch, P. S., Grossman, A., Tsu, T. T. & Imboden, J. B. (1988) *Eur. J. Immunol.* **18**, 525–532.
- Saizawa, K., Rojo, J. & Janeway, C. A., Jr. (1987) *Nature (London)* **328**, 260–263.
- Anderson, P., Blue, M.-L. & Schlossman, S. F. (1988) *J. Immunol.* **140**, 1732–1737.
- Rojo, J. M., Saizawa, K. & Janeway, C. A., Jr. (1989) *Proc. Natl. Acad. Sci. USA* **86**, 3311–3315.
- Mittler, R. S., Goldman, S. J., Spitalny, G. L. & Burakoff, S. J. (1989) *Proc. Natl. Acad. Sci. USA* **86**, 8531–8535.
- O'Neill, H. C., McGrath, M. S., Allison, J. P. & Weissman, I. L. (1987) *Cell* **49**, 143–151.
- Gallagher, P. F., de St. Groth, B. F. & Miller, J. F. A. P. (1989) *Proc. Natl. Acad. Sci. USA* **86**, 10044–10048.
- Tse, D. B. & Pernis, B. (1984) *J. Exp. Med.* **159**, 193–207.
- Oetgen, H. C., Pettey, C. L., Maloy, W. L. & Terhorst, C. (1986) *Nature (London)* **320**, 272–275.
- Damjanovich, S., Trón, L., Szöllösi, J., Zidovetzki, R., Vaz, W. L. C., Regateiro, F., Arndt-Jovin, D. J. & Jovin, T. M. (1983) *Proc. Natl. Acad. Sci. USA* **80**, 5985–5989.
- Szöllösi, J., Damjanovich, S., Goldman, C. K., Fulwyler, M. J., Aszalos, A. A., Goldstein, G., Rao, P., Talle, M. A. & Waldmann, T. A. (1987) *Proc. Natl. Acad. Sci. USA* **84**, 7246–7250.
- Davies, A. A., Cantrell, D. A., Hexham, J. M., Parker, P. J., Rothbard, J. & Crumpton, M. J. (1987) *J. Biol. Chem.* **262**, 10918–10921.
- Klausner, R. D., O'Shea, J. J., Luong, H., Ross, P., Bluestone, J. A. & Samelson, L. E. (1987) *J. Biol. Chem.* **262**, 12654–12659.
- Hoxie, J. A., Matthews, D. M., Callahan, K. J., Cassel, D. L. & Cooper, R. A. (1986) *J. Immunol.* **137**, 1194–1201.
- Krangel, M. S. (1987) *J. Exp. Med.* **165**, 1141–1159.
- Sibley, D. R., Benovic, J. L., Caron, M. G. & Lefkowitz, R. J. (1987) *Cell* **48**, 913–922.
- Fairclough, R. H. & Cantor, C. R. (1978) *Methods Enzymol.* **48**, 347–379.
- Cantor, C. R. & Pechukas, P. (1971) *Proc. Natl. Acad. Sci. USA* **68**, 2099–2101.
- Nisonoff, A., Hopper, J. E. & Spring, S. B. (1975) *The Antibody Molecule* (Academic, New York), pp. 209–237.
- Bray, D. & White, J. G. (1988) *Science* **239**, 883–888.
- Sheetz, M. P., Turney, S., Qian, H. & Elson, E. L. (1989) *Nature (London)* **340**, 284–288.
- Haft, D. & Eddin, M. (1989) *Nature (London)* **340**, 262–263.
- Janeway, C. A., Jr. (1989) *Immunol. Today* **10**, 234–238.
- Diamond, D. C., Sleckman, B. P., Gregory, T., Lasky, L. A., Greenstein, J. L. & Burakoff, S. J. (1988) *J. Immunol.* **141**, 3715–3717.
- Weinhold, K. J., Lyerly, H. K., Stanley, S. D., Austin, A. A., Matthews, T. J. & Bolognesi, D. P. (1989) *J. Immunol.* **142**, 3091–3097.
- Hoxie, J. A., Rackowski, J. L., Haggarty, B. S. & Gaulton, G. N. (1988) *J. Immunol.* **140**, 786–795.
- Bank, I. & Chess, L. (1985) *J. Exp. Med.* **162**, 1294–1303.